



ELSEVIER

Contents lists available at ScienceDirect

Journal of Luminescence

journal homepage: www.elsevier.com/locate/jlumin

Full Length Article

Kinetic energy dependence of carrier diffusion in a GaAs epilayer studied by wavelength selective PL imaging

S. Zhang^{a,b}, L.Q. Su^a, J. Kon^a, T. Gfroerer^c, M.W. Wanlass^{d,1}, Y. Zhang^{a,*}^a University of North Carolina at Charlotte, Charlotte, NC 28223, USA^b Providence High School, Charlotte, NC 28270, USA^c Davidson College, Davidson, NC 28035, USA^d National Renewable Energy Laboratory, Golden, CO 80401, USA

ARTICLE INFO

Article history:

Received 22 October 2016

Received in revised form

9 December 2016

Accepted 15 January 2017

Available online 18 January 2017

Keywords:

Photoluminescence imaging

Electron diffusion

Thermal distribution

Diffusion length

GaAs thin film

ABSTRACT

Photoluminescence (PL) imaging has been shown to be an efficient technique for investigating carrier diffusion in semiconductors. In the past, the measurement was typically carried out by measuring at one wavelength (e.g., at the band gap) or simply the whole emission band. At room temperature in a semiconductor like GaAs, the band-to-band PL emission may occur in a spectral range over 200 meV, vastly exceeding the average thermal energy of about 26 meV. To investigate the potential dependence of the carrier diffusion on the carrier kinetic energy, we performed wavelength selective PL imaging on a GaAs double hetero-structure in a spectral range from about 70 meV above to 50 meV below the bandgap, extracting the carrier diffusion lengths at different PL wavelengths by fitting the imaging data to a theoretical model. The results clearly show that the locally generated carriers of different kinetic energies mostly diffuse together, maintaining the same thermal distribution throughout the diffusion process. Potential effects related to carrier density, self-absorption, lateral wave-guiding, and local heating are also discussed.

© 2017 Elsevier B.V. All rights reserved.

1. Introduction

Photoluminescence (PL) imaging has been shown to be a very useful technique for investigating carrier diffusion in semiconductors [1–10]. Conceptually, the most straightforward and most widely adopted approach is using a tightly focused laser beam to generate carriers locally, then imaging the spatial distribution of the PL signal in the vicinity of the illumination site to probe the carrier diffusion. When the measurement is done in a time-resolved mode, the carrier diffusivity D can be extracted [1–5]. If the measurement is performed in a CW mode, one can instead extract the carrier diffusion length L that is related to D through $L = \sqrt{D\tau}$, where τ is the carrier lifetime that needs to be measured separately. A similar approach has also been used with cathodoluminescence (CL) where an electron beam is used to generate the carriers locally [11]. A complementary approach, which does not require the use of a focused laser beam, has also been demonstrated, by applying uniform illumination to the sample and using an isolated extended defect (typically a

dislocation) as a negative point source of generation [7,10]. Ideally, this defect should exhibit strong non-radiative recombination such that the PL at the defect site is strongly quenched. Yet another approach is to use a focused laser beam to scan near an isolated defect, where the PL signal is the combined effect of both a positive and negative point source of generation [8,10]. In these studies, often the PL signal of a single wavelength or a small band width near the band gap was probed [1–4,6,8–10], although sometimes the PL signal of the whole emission band was collected [5,7,11]. For a semiconductor like GaAs, the PL emission band at room temperature covers more than 200 meV [4], reflecting the contribution of carriers with very different kinetic energies [12]. One would like to ask: will the carriers of different kinetic energies diffuse together from the illumination site or equivalently will the thermal distribution remain the same during the carrier diffusion? This is a question of both fundamental and practical importance, as it is relevant to both the meaning of the extracted diffusion length from the PL imaging data and how the photo-generated carriers can be collected most efficiently in a solar cell. Surprisingly, this issue has not been explicitly examined.

In this work, we examined this problem using a high quality GaAs epilayer by performing wavelength selective PL imaging using the standard approach in the CW mode. We find that the carrier

* Corresponding author.

E-mail address: yong.zhang@uncc.edu (Y. Zhang).¹ Currently Wanlass Consulting.

diffusion lengths extracted from different emission energies in a range of about 50 meV below to 70 meV above the bandgap are approximately the same, implying the electrons and holes with kinetic energies significantly above or below the respectively band edge remain in thermal equilibrium while diffusing.

2. Material and methods

The sample was grown by metal-organic vapor phase epitaxy (MOVPE) on a semi-insulating GaAs substrate in a lattice-matched double heterostructure of GaInP/GaAs/GaInP. In such a double heterostructure, the photo-generated carriers can be confined within the thin GaAs layer between the energy barriers provided by GaInP layers, which also serve the purpose of passivating the dangling bonds of the GaAs surface and thus eliminating surface recombination [3,8]. Also, the carrier diffusion can be approximated as two-dimensional (2-D) lateral motion [3]. Specifically, the GaAs layer was 2 μm thick and nominally undoped with a n-type background doping level $\sim 5 \times 10^{14} \text{ cm}^{-3}$; the GaInP barrier layers were 100 nm thick, with the whole bottom barrier and the lower half (i.e., 50 nm) of the top barrier being nominally undoped, but the upper half of the top barrier being n-type doped at a level of $5 \times 10^{18} \text{ cm}^{-3}$. This sample was shown to have a very low as-grown threading dislocation density on the order of 10^3 cm^{-2} , as examined using a large area PL imaging technique [7] in order to locate the defects for studying carrier diffusion near individual defects [10].

The measurements were conducted at room temperature on a modified Horiba LabRAM HR800 confocal Raman microscope. The system was not designed for the intended measurements, since we sought to image the PL intensity distribution in a spatial range well beyond the laser illumination site, and the system can only measure the signal of the illumination site in the standard confocal mode. Therefore, the imaging camera, which is normally used for monitoring and visually examining the sample, was used to capture the PL image. We made an adaptor for holding filters and mounted it in the optical path to the camera. To accomplish the wavelength selection, a bandpass filter was placed on the adaptor before the camera. A bandpass filter of 10 nm bandwidth allowed only a narrow bandwidth of light to pass through while blocking other wavelengths of the PL signal from reaching the camera. Additionally, a notch filter at the excitation wavelength was added to further reduce the scattered laser light. A Torus 100 mW 532 nm laser (Laser Quantum) was used for excitation. A 100x microscope lens with numerical aperture $\text{NA} = 0.9$ was used for both laser focusing and signal collection with a corresponding Abbe diffraction limit spot size of $1.22\lambda/\text{NA} \approx 0.72 \mu\text{m}$. The image size was approximately $30 \mu\text{m} \times 30 \mu\text{m}$. The laser intensity was varied by either inserting a neutral density filter or changing the laser operation current. The typical laser power used for imaging was about 1 mW or $250 \text{ kW}/\text{cm}^2$. The imaging camera was an 8-bit color camera with 256 intensity scales; thus, the dynamic range was somewhat limited, which prevented us from analyzing very weak signals far away from either the bandgap (energetically) or the excitation site (spatially). Typically, 3–5 images were averaged for each wavelength, and background signal was removed by subtracting an image taken in the dark.

3. Results

Fig. 1 shows a 3-D PL image taken with an 830 nm bandpass filter, along with a typical PL spectrum taken at the same power in the confocal mode. The spectral windows of a few bandpass filters are indicated on the spectrum. The room temperature excitonic

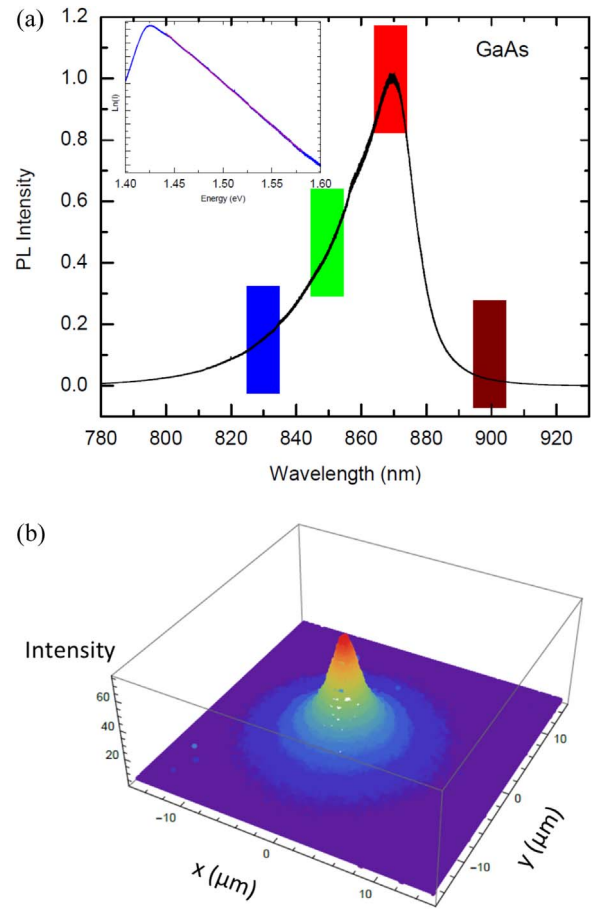


Fig. 1. A typical PL spectrum and PL image for a high quality GaAs epilayer. (a) A PL spectrum with four imaging spectral windows indicated. The inset shows a semi-logarithmic plot of the PL intensity vs. energy (in blue) with a solid line (in red) of a Boltzmann fit. (b) 3-D plot of a PL image at 830 nm generated by a focused 532 nm laser at the center (0,0).

bandgap of GaAs is $E_{\text{gx}} = 1.425 \text{ eV}$ (870 nm) [13]. The inset of Fig. 1 (a) shows a semi-logarithmic plot of the PL intensity versus energy. Because the high energy side is expected to follow the Boltzmann expression under the approximation of the band-to-band transition, $I(E) \propto \exp(-E/kT)$, where E is the emission energy [12], the slope can offer an estimate for the excitation site lattice temperature, which was found to be around 370 K, suggesting moderate local heating.

We analyzed PL images at four representative wavelengths, 830, 850, 870, and 900 nm, where the first two were ~ 68 and ~ 33 meV above the bandgap, and the last one ~ 48 meV below the bandgap. Fig. 2 shows normalized PL images in 2-D density plots at two power levels: (a) and (b) for 870 and 850 nm under ~ 1 mW power, and (c) and (d) for 870 nm and 900 nm under ~ 10 mW power (the 900 nm signal was too weak to measure at ~ 1 mW). The 870 nm images were taken under two power levels because the diffusion length was found to be excitation density dependent [8]. Dark counts were subtracted in the plots.

Fig. 3 plots the normalized and angularly averaged radial variation of the PL intensities at the four wavelengths. Fig. 3(a) and (b) are for the 1 mW and 10 mW results, respectively. It appears that the wavelength dependence is quite small. The radial dependence of the carrier density $n(r)$ in the 2-D approximation can be described by a modified Bessel function as $n(r) = G/(2\pi D) K_0(r/L)$ [10,11,14], where G is the generation rate of a delta function source at $r = 0$. Interestingly, this radial dependence is different from the Gaussian profile for the similar but time-dependent

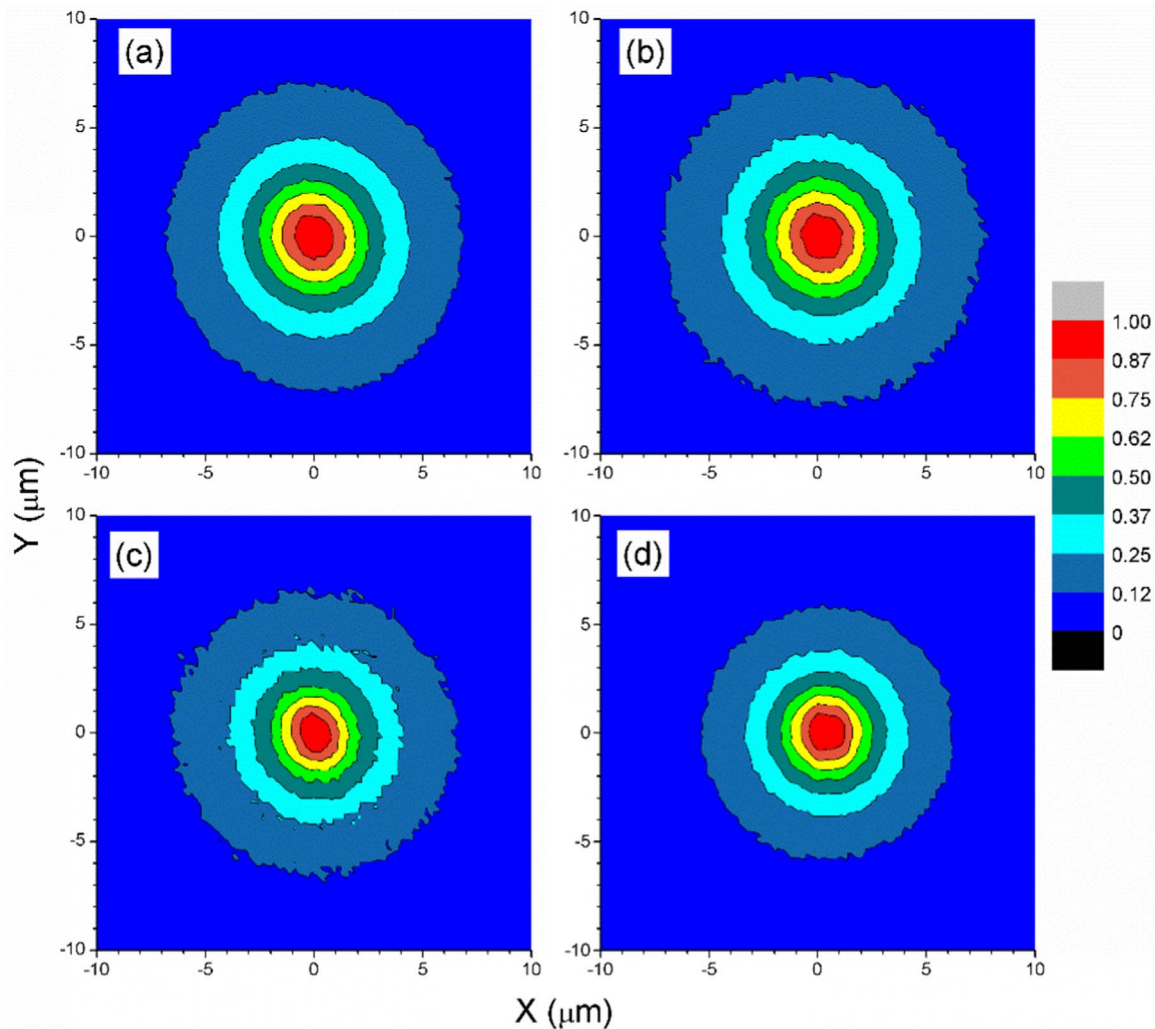


Fig. 2. Normalized two-dimensional (2-D) PL images. (a) and (b) for 870 and 850 nm, respectively, under ~ 1 mW power excitation; (c) and (d) for 870 nm and 900 nm under ~ 10 mW excitation.

problem [3]. The Bessel function solution $K_0(r/L)$ is divergent, though integrable, as $r \rightarrow 0$ if the excitation source is truly a delta function. However, when the excitation source has a finite size, the solution of the diffusion equation will be finite at the origin, and approach the Bessel function solution slightly away from the origin [10,14]. To avoid the complications very close to the excitation site related to the divergence of the Bessel function and the knowledge of the exact excitation profile as well as other considerations to be discussed later, we skipped the first few data points (within approximately twice the laser spot size) and fitted the radial dependence with $\alpha K_0(r/L)$, where L is the diffusion length and α is a constant. The fitted curves are shown in Fig. 3 (c) and (d) for comparison with the experimental data. We obtain diffusion lengths for the four wavelengths as 4.6, 4.8, and 4.8 μm for 830, 850, and 870 nm, respectively, under ~ 1 mW excitation, and 4.2 and 3.8 μm for 870 and 900 nm, respectively, under ~ 10 mW excitation. For 870 nm, the small reduction in diffusion length with increasing power is consistent with previous results [8,10]. The detailed fitting results are summarized in Table 1. For wavelengths from the bandgap 870 nm down to 830 nm, which covers most of the GaAs PL spectrum at room temperature, the PL signals yield similar diffusion lengths; for wavelengths from 870 nm up to 900 nm, there is a small reduction in diffusion length, but the intensity at 900 nm is insignificant relative to the total intensity. Therefore, broad band or single band detection

would not significantly affect the result for this sample. However, we emphasize that this conclusion is likely only valid for materials with minimal emission below the band gap, i.e., the PL emission is largely intrinsic interband recombination, such that the band edges serve as bottle necks for carrier thermalization. If below bandgap recombination from impurity or defect states with binding energies $\gg kT$ is significant, carriers in the conduction and valence bands may not be able to achieve quasi-equilibrium. The slightly reduced diffusion length at 900 nm compared to 870 nm might be an indication of the involvement of some impurity states. It will be of great interest in the future to examine the weaker signals further away from either the bandgap or the excitation site after improving the experimental setup and also carrying out the time-dependent study.

4. Discussion

The above treatment of the diffusion problem was based on the commonly adopted assumption of constant diffusion length or diffusivity and carrier lifetime so that the diffusion equation can be solved analytically [1–10]. Strictly speaking, the diffusion length depends on the carrier density, as found in previous work near a defect [8,10] as well as in this work in the defect free area. Therefore, the derived diffusion length should be viewed as an

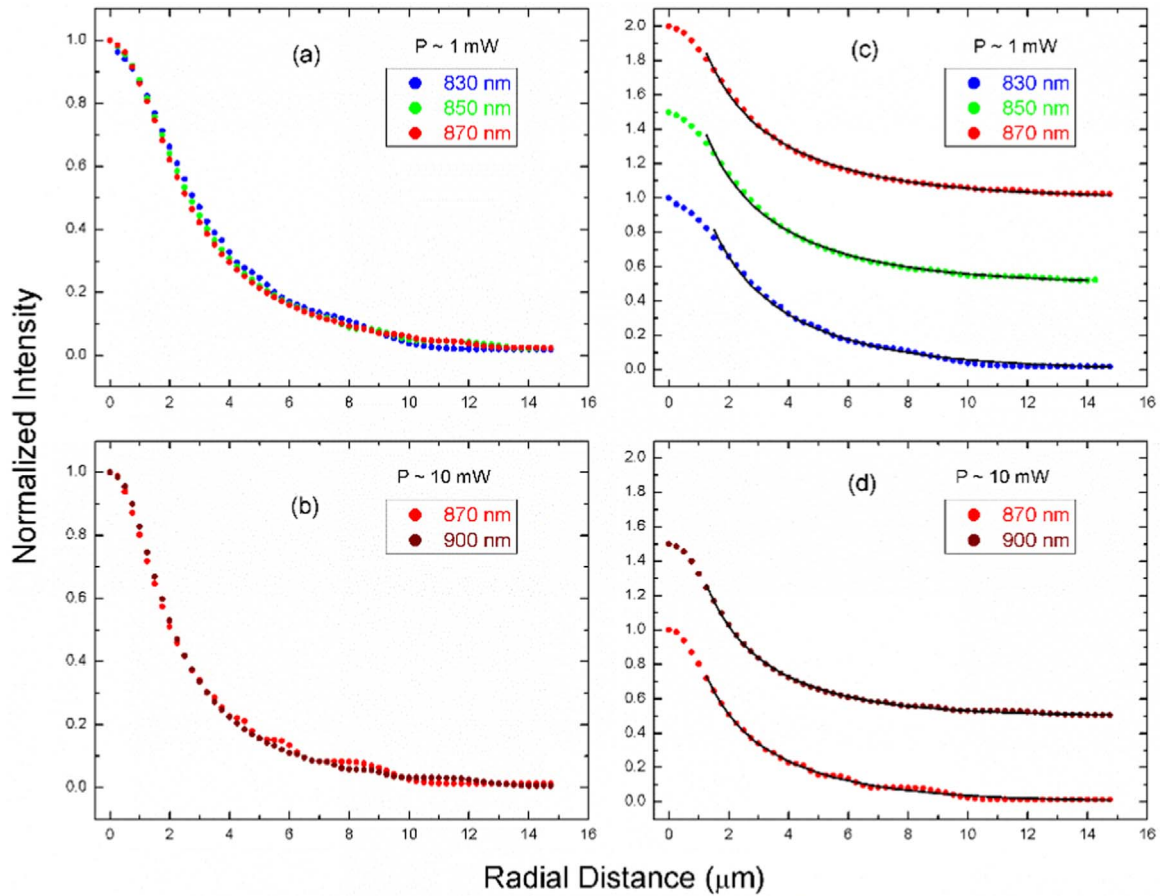


Fig. 3. Normalized and angularly averaged radial variation of the PL intensities. (a) and (b) are obtained from the PL imaging data of the 1 mW and 10 mW excitation, respectively; (c) and (d) show the comparison between the experimental data and the fitting results, corresponding to (a) and (b), respectively. The curves are shifted vertically for clarity.

Table 1
Fitting parameters.

P (mW)	~1			~10		
	λ (nm)	830	850	870	870	900
L (μm)		$4.63^{+0.20}_{-0.14}$	$4.79^{+0.24}_{-0.16}$	$4.77^{+0.21}_{-0.12}$	$4.16^{+0.08}_{-0.04}$	$3.78^{+0.11}_{-0.05}$
α		$0.626^{+0.030}_{-0.035}$	$0.576^{+0.027}_{-0.035}$	$0.563^{+0.020}_{-0.032}$	$0.532^{+0.007}_{-0.014}$	$0.592^{+0.012}_{-0.024}$

effective diffusion length. However, this approximation does not affect the qualitative conclusion of this work regarding wavelength dependence. Because the GaAs layer was slightly n-type due to residual background and top barrier doping, the diffusion length should be considered as the diffusion length of minority carriers – holes, and the values are consistent with those expected in a relatively high quality GaAs epilayer [3,4,8].

Although the 2-D approximation has been widely used in the literature for comparable or even thicker active layers (e.g., Refs [4,11]), a rigorous justification is non-trivial. Since the thickness of 2 μm is about twice of the absorption length (assuming $\alpha \sim 10^4 \text{ cm}^{-1}$), the use of the 2-D mode would seem not to be a good approximation. However, if the blurring in depth of focus caused by refractive index mismatch is taken into account, the carrier generation within the 2 μm GaAs layer is expected to be more uniform than that simply determined by the absorption law [15]. Furthermore, the existence of the bottom barrier will also help to establish a more uniform carrier distribution along the depth direction in the active layer [16]. For the primary purpose of

this work, the accuracy of the 2-D model is less important than in the other cases where the intent was to measure the diffusion length, here it is more important for us to determine whether or not the spatial profiles of different wavelengths are the same, regardless if the 2D model can accurately describe the profile.

The validity of the PL imaging technique is based on the assumption that the PL signal distribution is directly proportional to the carrier distribution. However, photon recycling has been mentioned as a potential concern in this type of measurement [17]. Because in the normal measurement condition only a small fraction of emitted light can escape from the front surface and be collected, the laterally directed PL signal could potentially obscure the real carrier diffusion. For emission with energy greater than E_{gx} , the strong absorption ($\alpha > 10^4 \text{ cm}^{-1}$) indicates that re-absorbed light will only affect the carrier distribution in a range roughly the size of the excitation beam, which effectively increases the beam size and should not be a major issue if the data in this region is neglected in the analysis (as in our analyses). For emission with energy below E_{gx} , for instance, the 1.377 eV (900 nm) emission, the absorption coefficient is expected to be rather small ($\alpha \sim 5 \times 10^2 \text{ cm}^{-1}$) [18], and the emitted light could in principle travel laterally over a distance exceeding 200 μm. Nevertheless, it will not escape through the front surface due to dielectric confinement, unless it encounters a major scattering center, such as the edge of a single crystalline sample or a domain boundary in a polycrystalline material. In fact, the diffusion length at 900 nm was found to be shorter than that of 870 nm, indicating that the effect of photon recycling was minimal. Not using the data points in the vicinity of the excitation site also avoided the local heating effect

caused by the tightly focused laser beam. To summarize, there are multiple practical reasons to skip the first few data points in the data fitting to avoid these complications: (1) the divergence difficulty of the modified Bessel function; (2) the complication of carrying out a numeral simulation with real laser profile; (3) the local heating effect at the excitation site; (4) the reabsorption effect of the emitted light in the vicinity of the excitation site.

5. Conclusions

In summary, we performed wavelength selective PL imaging measurements for an epitaxial GaAs sample, and showed that in a high quality sample, carriers with different kinetic energies mostly diffuse together, retaining the same energy distribution profile as they spread out into adjacent, lower-concentration regions.

Acknowledgement

The authors would like to thank J. J. Carapella for performing the MOVPE growth. Funding: This work was supported by ARO/MURI (W911NF-10-1-0524, Dr. William Clark), ARO/Electronics (W911NF-16-1-0263, Dr. William Clark), and Bissell Distinguished Professorship.

References

- [1] A. Olsson, D.J. Erskine, Z.Y. Xu, A. Schremer, C.L. Tang, Nonlinear luminescence and time-resolved diffusion profiles of photoexcited carriers in semiconductors, *Appl. Phys. Lett.* 41 (1982) 659.
- [2] D.P. Trauernicht, J.P. Wolfe, Drift and diffusion of paraexcitons in Cu_2O : deformation-potential scattering in the low-temperature regime, *Phys. Rev. B* 33 (1986) 8506.
- [3] G.D. Gilliland, D.J. Wolford, T.F. Kuech, J.A. Bradley, Long-range, minority-carrier transport in high quality "surface-free" GaAs/AlGaAs double heterostructures, *Appl. Phys. Lett.* 59 (1991) 216.
- [4] D.J. Wolford, G.D. Gilliland, T.F. Kuech, J.A. Bradley, H.P. Hjalmarson, Optically determined minority-carrier transport in GaAs/ $\text{Al}_x\text{Ga}_{1-x}\text{As}$ heterostructures, *Phys. Rev. B* 47 (1993) 15601.
- [5] B. Fluegel, K. Alberi, M.J. DiNezza, S. Liu, Y.H. Zhang, A. Mascarenhas, Carrier Decay and diffusion dynamics in single-crystalline cdtc as seen via micro-photoluminescence, *Phys. Rev. Appl.* 2 (2014) 034010.
- [6] W. Bao, M. Melli, N. Caselli, F. Riboli, D.S. Wiersma, M. Staffaroni, H. Choo, D. F. Ogletree, S. Aloni, J. Bokor, S. Cabrini, F. Intonti, M.B. Salmeron, E. Yablonovitch, P.J. Schuck, A. Weber-Bargioni, Mapping local charge recombination heterogeneity by multidimensional nanospectroscopic imaging, *Science* 338 (2012) 1317.
- [7] T.H. Gfroerer, C.M. Crowley, C.M. Read, M.W. Wanlass, Excitation-dependent recombination and diffusion near an isolated dislocation in GaAs, *J. Appl. Phys.* 111 (2012) 093712.
- [8] T.H. Gfroerer, Y. Zhang, M.W. Wanlass, An extended defect as a sensor for free carrier diffusion in a semiconductor, *Appl. Phys. Lett.* 102 (2013) 012114.
- [9] K. Alberi, B. Fluegel, H. Moutinho, R.G. Dhere, J.V. Li, A. Mascarenhas, Measuring long-range carrier diffusion across multiple grains in polycrystalline semiconductors by photoluminescence imaging, *Nat. Commun.* 4 (2013).
- [10] F. Chen, Y. Zhang, T.H. Gfroerer, A.N. Finger, M.W. Wanlass, Spatial resolution versus data acquisition efficiency in mapping an inhomogeneous system with species diffusion, *Sci. Rep.* 5 (2015).
- [11] N.M. Haegel, T.J. Mills, M. Talmadge, C. Scandrett, C.L. Frenzen, H. Yoon, C. M. Fetzer, R.R. King, Direct imaging of anisotropic minority-carrier diffusion in ordered GaInP, *J. Appl. Phys.* 105 (2009) 023711.
- [12] H.B. Bebb, E.W. Williams, Transport and optical phenomena, in: R.K. Willardson, A.C. Beer (Eds.), *Photoluminescence I: Theory*, Academic Press, New York, 1972, p. 181.
- [13] Y. Zhang, B. Fluegel, M. Hanna, A. Duda, A. Mascarenhas, Materials research society symposium proceedings, in: E.D. Jones et al. (Ed.), *Electronic Structure near the Band Gap of Heavily Nitrogen Doped GaAs and GaP*, MRS, Warrendale, 2001, p. 49.
- [14] C. Donolato, Modeling the effect of dislocations on the minority carrier diffusion length of a semiconductor, *J. Appl. Phys.* 84 (1998) 2656.
- [15] N.J. Everall, Confocal Raman microscopy: why the depth resolution and spatial accuracy can be much worse than you think, *Appl. Spectrosc.* 54 (2000) 1515.
- [16] R.K. Ahrenkiel, B.M. Keyes, G.B. Lush, M.R. Melloch, M.S. Lundstrom, H. F. MacMillan, Minority-carrier lifetime and photon recycling in n-GaAs, *J. Vac. Sci. Technol. A* 10 (1992) 990.
- [17] G.D. Gilliland, D.J. Wolford, T.F. Kuech, J.A. Bradley, H.P. Hjalmarson, Minority-carrier recombination kinetics and transport in "surface-free" GaAs/ $\text{Al}_x\text{Ga}_{1-x}\text{As}$ double heterostructures, *J. Appl. Phys.* 73 (1993) 8386.
- [18] M.D. Sturge, Optical absorption of gallium arsenide between 0.6 and 2.75 eV, *Phys. Rev.* 127 (1962) 768.